Applied Surface Science Advances 13 (2023) 100367

Contents lists available at ScienceDirect

Applied Surface Science Advances

journal homepage: www.sciencedirect.com/journal/applied-surface-science-advances

Synthesis and characterization and X-ray/gamma ray absorption properties of tin oxide synthesized via solution combustion method

Y.S. Uday [a], Y.S. Vidya [b,*], H.C. Manjunatha [c,*], S. Manjunath [d], K.N. Sridhar [c], Nagashree K . L [d]

[a] Department of Chemistry, Sri Lakshmi PU College, Sunkadakatte, Magadi Road, Vishwaneedham Post, Bangalore, Karnataka 560091, India
[b] Department of Physics, Lal Bahadur Shastri Government First Grade College, RT Nagar, Bangalore, Karnataka 560032, India
[c] Department of Physics, Government College for women, Kolar, Karnataka 563101, India
[d] Department of Chemistry, B.M.S College of Engineering, Bengaluru, Karnataka 560019, India

ARTICLE INFO

Keywords:
SnO_2
Solution combustion method
Mass attenuation coefficient
Nanoparticle

ABSTRACT

Tin oxide (SnO_2) nanoparticles (NPs) are synthesized via solution combustion method using Glycine as a fuel followed by the calcination and characterization. The Bragg reflections clearly confirms the formation of tetragonal rutile phase with crystallite size 10 nm. The irregular shaped agglomerated NPs are observed on the surface morphology. The energy band gap was determined (3.7 eV). Theoretically, mass attenuation coefficient is determined which is an essential data required in diverse fields.

1. Introduction

Transition metal oxides are inexpensive, versatile and stable at high temperatures and finds an application as a photocatalyst, sensor and other different fields. These transition metal oxides possess range of electrical properties from insulators to superconducting property [1]. Transition metal oxides possess high electrochemical activities and contribute to high capacitance. The oxides / composites obtained from these metals shows well defined morphology, surface / interface properties, good mechanical properties etc., [2]. The MgO-ZrO_2 composites finds an industrial application in manufacturing gas turbine blades [3]. However, MnO_2, has gained the attention of researchers in the field of biosensing and biomedical [4].

Among the different transition metal oxide, Tin dioxide is a key component for optoelectronic applications since it is one of a class of materials with excellent electrical conductivity and optical transparency. Tin oxide is being studied because it can be used as a transparent conductor [5], photocatalyst [6], and solid state gas sensor [7], Lithium ion batteries [8] etc. Yuan and Xu [9] synthesized SnO_2 at nanolevel and studied the photocatalytic properties for the decolorization of Methyl Orange dye. Li et.al. [10] studied the performance of SnO_2 for NO_2 sensor.

Ionizing radiation is being used more frequently in business, agriculture, medicine and energy. Nevertheless, despite the numerous advantages of using these rays, extreme caution must be exercised due to the potential hazards of exposure [11]. Utilizing radiation shielding to protect the user from exposure to high radiation levels is one of the most crucial safety measures. Now-a-days number of research work has been carried out in searching of new and efficient shielding materials alternative lead materials as it is toxic to the environment [12,13]. The usual shielding focuses on the use of standard metals / composites / polymers etc. But they suffer from some drawbacks such as poor mechanical properties and complicated binder preparation etc. On the other hand semiconductors with wide band gap are more stable than polymers and they possess good mechanical strength required for the shielding purpose [14]. Number of research work has been carried out on the shielding properties of on different materials containing SnO_2, [15–17]. But until now, research work on the shielding properties of SnO_2 are very few.

Various techniques such as Mechanochemical [18], thermolysis [19], sol-gel [20], molten salt [21], co-precipitation [22] shell-by-shell synthesis [23] etc. Among all these methods, solution combustion method is a novel, fast, economical, less time consuming and efficient method. Thus, in the present study, solution combustion method is used to synthesize SnO_2 NPs using Glycine as a fuel. Babu et.al. [24] synthesized Cobalt doped SnO_2 NPs by solution combustion method and investigated on structural and optical properties of host matrix by varying the dopant. Shajira et.al. [25] synthesized Mg doped SnO_2 NPs and studied the energy band structure of host matrix.

In the present communication, SnO_2 NPs are synthesized via facile,

* Corresponding authors.
E-mail addresses: vidyays.phy@gmail.com (Y.S. Vidya), manjunathhc@rediffmail.com (H.C. Manjunatha).

https://doi.org/10.1016/j.apsadv.2023.100367
Received 22 July 2022; Received in revised form 8 December 2022; Accepted 6 January 2023
Available online 12 January 2023

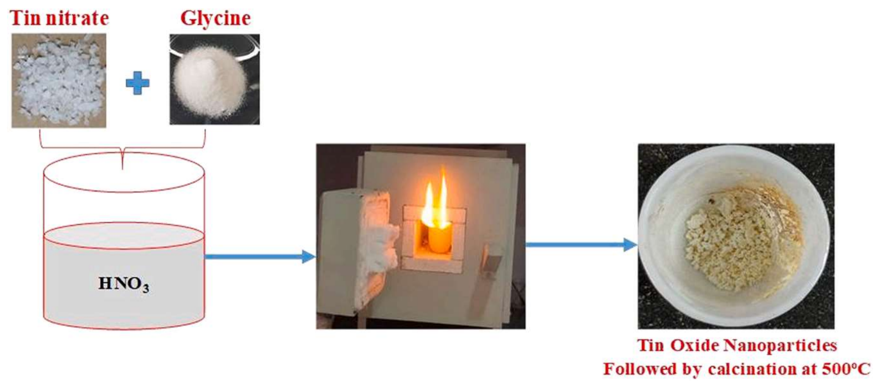

Fig. 1. Flowchart for the synthesis of SnO_2 NPs.

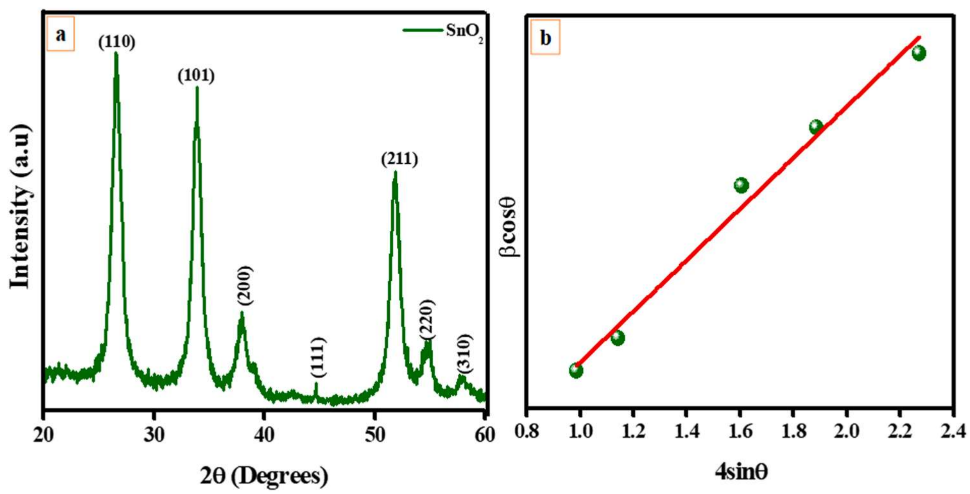

Fig. 2. (a) PXRD pattern and (b) W-H plot of SnO_2 NPs.

economical solution combustion method using Glycine as a fuel followed by calcination at 500°C for 3 h. The calcined samples are well characterized with different techniques. The X-ray/gamma ray radiation shielding properties are discussed in detail where the matrix finds an application in a radiation shielding as a good radiation absorber.

2. Materials and methods

2.1. Synthesis of SnO_2 NPs

Tin nitrate is the source of tin oxide. Stoichiometric amount of tin nitrate (dissolved in minimum amount of nitric acid) and Glycine as a fuel. This mixture is subjected to combustion followed by the calcination at 500°C for 3h. The flowchart for the synthesis of SnO_2 NPs is shown in Fig. 1.

2.2. Characterization of SnO_2 NPs

The synthesized NPs were characterized using Shimadzu Powder X-ray diffractometer (PXRD). The diffraction patterns were recorded at room temperature using Cu K_α (1.541 Å) radiation with nickel filter in the 2h range 20–70° at a scan rate of 2° min^{-1}. The surface morphology were studied by scanning electron microscopy (SEM, Hitachi-3000), Fourier Transform Infrared Spectroscopy (FTIR) studies were performed with a PerkinElmer Forntier FTIR spectrometer. The UV-Visible absorption spectrum was recorded on PerkinElmer spectrometer.

Table 1
Crystallite size and other structural parameters of SnO_2 NPs.

Sample	Crystallite size (nm)		Stress x 10^{-3}	Dislocation density x 10^{16} linm^{-2}	Structural factor
	Scherrer's	W-H			
SnO_2	16	18	1.587	3.906	0.5235

2.3. Theoretical evaluation of mass attenuation coefficient of SnO_2 nanoparticles

Theoretically, gamma ray shielding parameters such as Mass attenuation coefficient (μ/ρ) is calculated in the energy range 1 keV–1GeV and is computed by using WinXCom code [26,27].

3. Results and discussion

3.1. PXRD analysis of SnO_2 NPs

PXRD pattern of SnO_2 NPs recorded in the range 20–60° shows the Bragg's reflections at 26.8, 34.12, 37.88, 44.89, 51.84, 54.85 and 58° 2θ values corresponding to (110), (101), (200), (111), (211), (220) and (002) planes, respectively (Fig. 2a). No other impurity phases or peaks are observed. The PXRD pattern matches well with the JCPDS card No. 41-1445 [28] and confirms the formation of single tetragonal phase. The estimated crystallite size (Fig. 2b) and other structural parameters are tabulated in Table 1 [29].

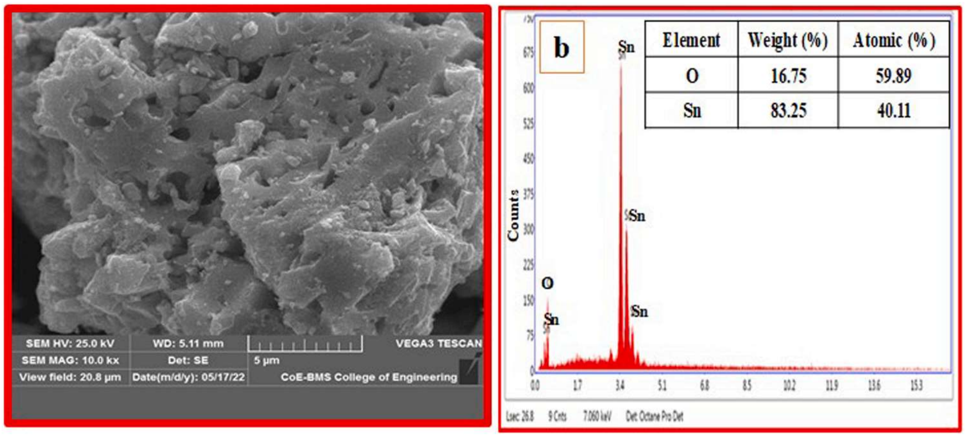

Fig. 3. (a) SEM image and (b) EDAX spectra (Inset: Atomic and weight percentage of elements) of SnO_2 NPs.

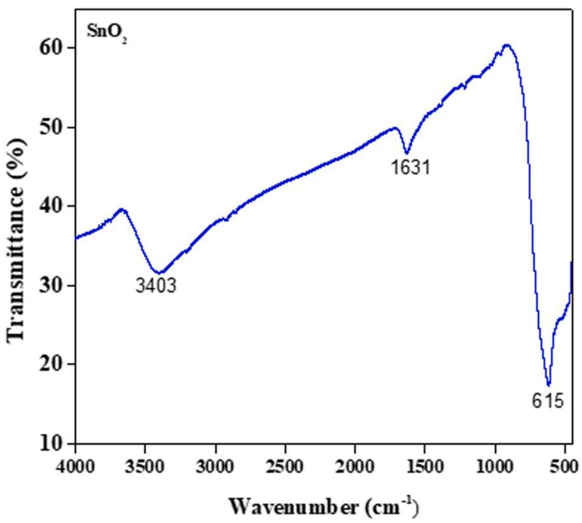

Fig. 4. FTIR spectra of SnO_2 NPs.

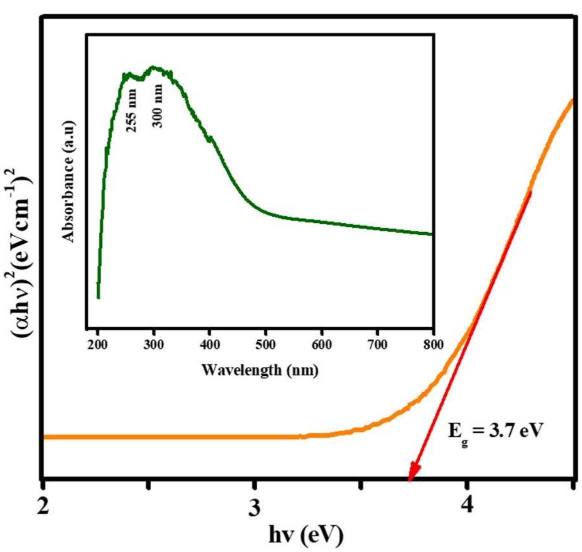

Fig. 5. The variation of $(\alpha h\nu)^2$ Vs $h\nu$ (UV-Visible spectra) of SnO_2 NPs.

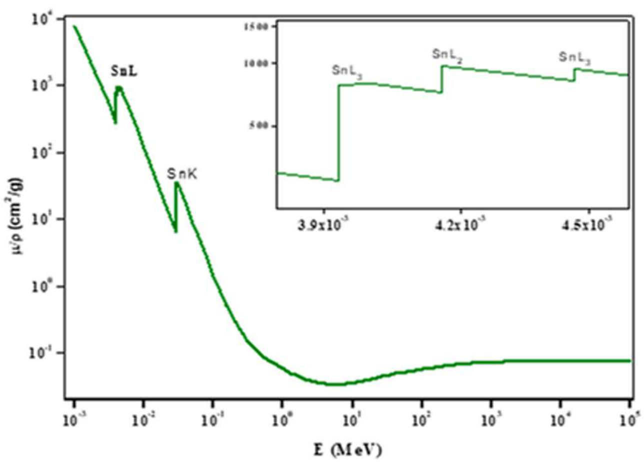

Fig. 6. Variation of variation of μ/ρ with gamma interaction energy.

3.2. SEM analysis of SnO_2 NPs

The surface morphology consists agglomerated irregular shaped NPs along with pores and hallows. These pores and hallows are the characteristics of combustion synthesized NPs (Fig. 3a). Fig. 3a and inset Table of Fig. 3b shows the recorded EDAX spectra and atomic weight fractions of SnO_2 NPs.

3.3. FTIR analysis of SnO_2 NPs

FTIR spectra was recorded for SnO_2 NPs. The absorption peak observed at 515 cm^{-1} corresponds to Metal-Oxygen bond whereas remaining two peaks corresponds to O-H vibrational modes of water molecule Fig. 4.

3.4. UV-Visible absorption spectroscopy analysis of SnO_2 NPs

The UV-Visible absorption spectra consists two absorption peaks located at 255 and 300 nm (Inset of Fig. 5). This broad absorption peak might be due to surface-related defects in SnO_2 NPs [30].By plotting the graph between $(\alpha h\nu)^2$ Vs $h\nu$ direct energy band gap was found to be 3.7 eV (Fig. 5).

3.5. Determination of X-rays/Gamma rays radiation shielding parameter of SnO_2 NPs

Among the different radiation shielding parameters, mass

Table 2
Comparison of mass attenuation of SnO_2, Tungsten, Lead and Concrete materials at different energies.

E (MeV)	SnO2 (Glycine)		Tungsten	Lead	Concrete
	Theoretical	Experimental			
0.276	0.187	0.212	0.324	0.403	0.109
0.356	0.131	0.165	0.193	0.232	0.098
0.511	0.091	0.092	0.138	0.161	0.089
0.6615	0.077	0.076	0.109	0.125	0.082
1.173	0.054	0056	0.056	0.059	0.058
1.332	0.051	0.053	0.05	0.052	0.053

attenuation coefficient (MAC) which plays an important role. Fig. 6 shows the variation of μ/ρ with the Gamma energy (1 keV–1 GeV). In general, different interaction process is dominant at different energy regions. Whenever, SnO_2 NPs interact with gamma rays, inner shell electrons absorb the energy and excited to higher energy levels. These excited electrons come to lower energy levels by emitting the X-rays at particular wavelength / energy. This energy gives rise to absorption edge which is the fingerprint of the particular element present in the sample. In the Fig. 6, it is clearly observed that, the interaction of 'Sn' with gamma radiation shows the X-ray absorption edges SnL3, SnL2, SnL1 and SnK at 3.93,4.16, 4.46 and 29.2 keV (Inset of Fig. 6). Eventhough, oxygen is present in the sample, because of its lower atomic number, its signature is not observed. Accurate values of MAC is an essential parameter which is required in diverse fields such as radiation protection. Comparison of mass attenuation of SnO_2 synthesized using Glycine as a fuel with Tungsten, Lead and Concrete materials at different energies are tabulated in Table 2.

3.6. Summary

In the present communication, SnO_2 NPs are synthesized via solution combustion method followed by the calcination at 500°C for 3 h and characterization. The procured samples are characterized with different techniques. The Bragg's reflections confirm the formation of tetragonal SnO_2 NPs with 16 nm crystallite size. The surface morphology consists irregular shaped NPs. The determined energy band gap was found to be 3.7 eV. Theoretically mass attenuation coefficient is determined which is an essential parameter in diverse fields such as radiation dosimetry, radiation physics, radiation engineering etc. Hence, the synthesized SnO_2 NPs especially helpful for shielding situations where it is advantageous to be in the radiation source's line of sight.

Declaration of Competing Interest

The authors declare the following financial interests/personal relationships which may be considered as potential competing interests: Not Applicable

References

[1] M. Batzill, U. Diebold, The surface and materials science of tin oxide, Prog. Surf. Sci. 79 (2-4) (2005) 47–154.
[2] C. Yuan, H.B. Wu, Y. Xie, X.W. Lou, Mixed transition-metal oxides: design, synthesis, and energy-related applications, Angew. Chem. Int. Ed. 53 (6) (2014) 1488–1504.
[3] L. Keerthana, C. Sakthivel, I. Prabha, Mgo-zro2 mixed nanocomposites: fabrication methods and applications, Mater. Today Sustain. 3 (2019), 100007.
[4] J. Chen, H. Meng, Y. Tian, R. Yang, D. Du, Z. Li, L. Qu, Y. Lin, Recent advances in functionalized mno 2 nanosheets for biosensing and biomedicine applications, Nanoscale Horiz. 4 (2) (2019) 321–338.
[5] Y.J. Seo, G.W. Kim, C.H. Sung, M.S. Anwar, C.G. Lee, B.H. Koo, Characterization of transparent and conductive electrodes of nb-doped SnO_2 thin film by pulsed laser deposition, Curr. Appl Phys. 11 (3) (2011) S310–S313.
[6] N.P. Moraes, C.M. Goes, D.C. Sperandio, R.S. Rocha, R. Lan-ders, T. Paramasivam, L.A. Rodrigues, Development of a new zinc oxide/tin oxide/carbon xerogel photocatalyst for visible light photodegradation of 4-chlorophenol, Mater. Sci. Eng. B 269 (2021), 115183.
[7] C. Li, M. Lv, J. Zuo, X. Huang, SnO_2 highly sensitive co gas sensor based on quasi-molecular- imprinting mechanism design, Sensors 15 (2) (2015) 3789–3800.
[8] J. Read, D. Foster, J. Wolfenstine, W. Behl, SnO_2-carbon composites for lithium-ion battery anodes, J. Power Sources 96 (2) (2001) 277–281.
[9] H. Yuan, J. Xu, Preparation, characterization and photocatalytic activity of nanometer SnO_2, Int. J. Chem. Eng. Appl. 1 (3) (2010) 241–246.
[10] Ji Li, M. Yang, X. Cheng, X. Zhang, C. Guo, Y. Xu, S. Gao, Z. Major, H. Zhao, L. Huo, Fast detection of no2 by porous SnO_2 nanotoast sensor at low temperature, J. Hazard. Mater. 419 (2021), 126414.
[11] S.A.M. Issa, H.M.H. Zakaly, M. Pyshkina, M.Y.A. Mostafa, M. Rashad, T.S. Soliman, Structure, optical, and radiation shielding properties of PVA–BaTiO3 nanocomposite films: an experimental investigation, Radiat. Phys. Chem. 180 (2021), 109281.
[12] K.M. Batoo, M. Hadi, R. Verma, A. Chauhan, R. Kumar, M. Singh, O.M. Aldossary, Improved microwave absorption and emi shielding properties of ba-doped Co–Zn ferrite, Ceram. Int. 48 (3) (2022) 3328–3343.
[13] M. Hadi, K.M. Batoo, A. Chauhan, O.M. Aldossary, R. Verma, Y. Yang, Tuning of structural, dielectric, and electronic properties of Cu doped Co–Zn ferrite nanoparticles for multilayer inductor chip applications, Magnetochemistry 7 (4) (2021) 53.
[14] S.M. Jeong, J. Ahn, Y.K. Choi, T. Lim, K. Seo, T. Hong, G.H. Choi, H. Kim, B.W. Lee, S.Y. Park, et al., Development of a wearable infrared shield based on a polyurethane–antimony tin oxide composite fiber, NPG Asia Mater. 12 (1) (2020) 1–13.
[15] M.A. Alothman, R. Kurtulus, I.O. Olarinoye, T. Kavas, C. Mutuwong, M.S. Al-Buriahi, Optical, elastic, and radiation shielding properties of Bi_2O_3-PBO-B_2O_3 glass system: a role of SnO_2 addition, Optik 248 (2021), 168047.
[16] Y.S. Rammah, M.I. Sayyed, A.S. Abohaswa, H.O. Tekin, Ftir, electronic polarizability and shielding parameters of B_2O_3 glasses doped with SnO_2, Appl. Phys. A 124 (9) (2018) 1–9.
[17] E. Hannachi, M.I. Sayyed, B. Albarzan, A.H. Almuqrin, K.A. Mahmoud, Synthesis and study of structural, optical and radiation-protective peculiarities of $MTiO_3$ (M= Ba, Sr) metatitanate ceramics mixed with SnO_2 oxide, Ceram. Int. 47 (20) (2021) 28528–28535.
[18] H. Yang, Y. Hu, A. Tang, J. Shengming, G. Qiu, Synthesis of tin oxide nanoparticles by mechanochemical reaction, J. Alloy. Compd. 363 (1-2) (2004) 276–279.
[19] C. Nayral, E. Viala, P. Fau, F. Senocq, J.C. Jumas, A. Maisonnat, B. Chaudret, Synthesis of tin and tin oxide nanoparticles of low size dispersity for application in gas sensing, Chem. Eur. J. 6 (22) (2000) 4082–4090.
[20] M. Marikkannan, V. Vishnukanthan, A. Vijayshankar, J. Mayandi, J.M. Pearce, A novel synthesis of tin oxide thin films by the sol-gel process for optoelectronic applications, AIP Adv. 5 (2) (2015), 027122.
[21] Y. Wang, J.Y. Lee, Molten salt synthesis of tin oxide nanorods: morphological and electrochemical features, J. Phys. Chem. B 108 (46) (2004) 17832–17837.
[22] S. Tazikeh, A. Akbari, A. Talebi, E. Talebi, Synthesis and characterization of tin oxide nanoparti- cles via the co-precipitation method, Mater. Sci. Pol. 32 (1) (2014) 98–101.
[23] X.W. Lou, C. Yuan, L.A. Archer, Shell-by-shell synthesis of tin oxide hollow colloids with nanoarchitectured walls: cavity size tuning and functionalization, Small 3 (2) (2007) 261–265.
[24] B. Babu, Ch Reddy, J. Shim, R. Ravikumar, J. Park, et al., Effect of cobalt concentration on morphol- ogy of co-doped SnO_2 nanostructures synthesized by solution combustion method, J. Mater. Sci. Mater. Electron. 27 (5) (2016) 5197–5203.
[25] P.S. Shajira, M. Junaid Bushiri, B.B. Nair, V. Ganeshchandra Prabhu, Energy band structure investigation of blue and green light emitting mg doped SnO_2 nanostructures synthesized by combustion method, J. Lumin. 145 (2014) 425–429.
[26] B. Chinnappa Reddy, H.C. Manjunatha, Y.S. Vidya, K.N. Sridhar, U. Mahaboob Pasha, L. Seenappa, B. Sadashivamurthy, N. Dhananjaya, K.V. Sathish, P. S. Damodara Gupta, X-ray/gamma ray radiation shielding properties of α-Bi_2O_3 synthesized by low temperature solution combustion method, Nucl. Eng. Technol. 54 (3) (2022) 1062–1070.
[27] A. Shivashankar, S.C. Prashantha, K.S. Anantharaju, S. Malini, H.C. Manjunatha, Y. S. Vidya, K.N. Sridhar, R. Munirathnam, Rod shaped zirconium titanate nanoparticles: Synthesis, comparison and systematic investigation of structural, photoluminescence, electrochemical sensing and supercapacitor properties, Ceram. Int. (2022).
[28] A. Debataraja, D.W. Zulhendri, B. Yuliarto, B. Sunendar, et al., Investigation of nanos- tructured SnO_2 synthesized with polyol technique for co gas sensor applications, Procedia Eng. 170 (2017) 60–64.
[29] J.B. Prasannakumar, Y.S. Vidya, K.S. Anantharaju, G. Ramgopal, H. Nagabhushana, S.C. Sharma, B. Daruka Prasad, S.C. Prashantha, R.B. Basavaraj, H. Rajanaik, et al., Bio-mediated route for the synthesis of shape tunable Y_2O_3: Tb^{3+} nanoparticles: photoluminescence and antibacterial properties, Spectrochim. Acta Part A 151 (2015) 131–140.
[30] R.N. Mariammal, K. Ramachandran, B. Renganathan, D. Sastikumar, On the enhancement of ethanol sensing by cuo modified SnO_2 nanoparticles using fiber-optic sensor, Sens. Actuators B 169 (2012) 199–207.